SCIENTIFIC REPORTS

OPEN

SUBJECT AREAS:
SYNTHESIS OF GRAPHENE
DESIGN, SYNTHESIS AND PROCESSING

Received
25 June 2014

Accepted
28 July 2014

Published
19 August 2014

Correspondence and requests for materials should be addressed to Z.W.P. (panz@uga.edu) or M.H. (mhildebrand@ucsd.edu)

* Current address: School of Mechanical Engineering, Shandong University, Jinan 250061, China.

† Current address: Center for Nanophase Materials Science, Oak Ridge National Laboratory, Oak Ridge, TN 37831, USA.

‡ Current address: Hitachi High-Technologies Canada Inc., 89 Galaxy Blvd, Suite 14, Toronto, ON M9W 6A4, Canada.

Electronically transparent graphene replicas of diatoms: a new technique for the investigation of frustule morphology

Zhengwei Pan[1,2], Sarah J. L. Lerch[3], Liang Xu[1]*, Xufan Li[1]†, Yen-Jun Chuang[1], Jane Y. Howe[4]‡, Shannon M. Mahurin[5], Sheng Dai[5] & Mark Hildebrand[3]

[1]College of Engineering, University of Georgia, Athens, GA 30602, USA, [2]Department of Physics and Astronomy, University of Georgia, Athens, GA 30602, USA, [3]Scripps Institution of Oceanography, University of California, San Diego, La Jolla, CA 92093, USA, [4]Materials Science and Technology Division, Oak Ridge National Laboratory, Oak Ridge, TN 37831, USA, [5]Chemical Science Division, Oak Ridge National Laboratory, Oak Ridge, TN 37831, USA.

The morphogenesis of the silica cell walls (called frustules) of unicellular algae known as diatoms is one of the most intriguing mysteries of the diatoms. To study frustule morphogenesis, optical, electron and atomic force microscopy has been extensively used to reveal the frustule morphology. However, since silica frustules are opaque, past observations were limited to outer and fracture surfaces, restricting observations of interior structures. Here we show that opaque silica frustules can be converted into electronically transparent graphene replicas, fabricated using chemical vapor deposition of methane. Chemical vapor deposition creates a continuous graphene coating preserving the frustule's shape and fine, complicated internal features. Subsequent dissolution of the silica with hydrofluoric acid yields a free-standing replica of the internal and external native frustule morphologies. Electron microscopy renders these graphene replicas highly transparent, revealing previously unobserved, complex, three-dimensional, interior frustule structures, which lend new insights into the investigation of frustule morphogenesis.

Diatoms – unicellular, eukaryotic, photosynthetic microalgae which are abundantly and ubiquitously present in all aquatic and moist environments and play crucial roles in a wide range of global issues (e.g., climate change, carbon cycle, marine ecosystem, *etc.*) – have fascinated numerous amateur diatomists and professional researchers for more than two centuries with a whole range of mysteries[1–10]. One of the most intriguing mysteries of the diatoms is the morphogenesis of their most conspicuous feature, the silica cell walls called frustules[4]. A frustule is shaped similarly to a Petri dish consisting of two valves joined with overlapping girdle bands. Each frustule features a three-dimensional (3D), intricately patterned, nanoscale, and species-specific silica structure. Classified by the shapes and patterned structures of the valves, there are more than 100,000 estimated diatom species[1–3]. Since the diatom cells interact with their external environment through the frustule walls, understanding the morphogenesis of the frustules, i.e., how diatoms make their intricately patterned silica shells, has important implications to the understanding of diatom biology and physiology[11]. To study frustule morphogenesis, optical, electron and atomic force microscopy has been extensively used to reveal the frustule morphologies and structures[1–3,12,13]. However, since silica frustules are opaque, past observations were limited to outer and fracture surfaces, restricting observations of interior structures.

In this study, we report a new technique for the observation of the interior structures of the diatom frustules. We converted opaque silica frustules into electronically transparent graphene replicas by using catalyst-free chemical vapor deposition (CVD) of methane, followed by dissolution of the silica with hydrofluoric acid. The graphene replicas precisely retain the external and internal native frustule morphology. Due to the thin, conductive nature of the graphene coating, electron microscopy renders the graphene replicas highly transparent. This enables, for the first time, the entire interior structures of a diatom frustule to be clearly visualized, and reveals previously unobserved, complex, 3D, interior frustule structures, providing new insights into the investigation of frustule morphogenesis. This study also establishes a metal-catalyst-free CVD method to grow quality graphene on silica surfaces.

Results

Morphologies of silica frustules and the making of graphene replicas. The frustules used in this study were obtained from a sample of diatomaceous earth which was treated to remove impurities and debris before CVD. The frustules were mainly produced by two species of diatoms belonging to the genus *Aulacoseira*[1] (Supplementary Fig. 1). These two dominant species were defined by frustule morphologies and fine features. One species' frustule shows rows of areolae (i.e., pores; ~500 nm in diameter) running parallel to the valve axes (Fig. 1a,b). These areolae are shaped like circular, continuous, cylindrical channels which penetrate into the frustule's interior. We refer to this species as species *A*1. The second species has slightly dextrorse curving rows of areolae (Fig. 1c,d). The areolae are shaped like elongated ovals which open into a seemingly porous frustule wall (Supplementary Fig. 2). Across the opening of these areolae is a distinct submicron network of fine, interconnected silica nanorods (50−100 nm in diameter) creating a mesh (Fig. 1e). We refer to this species as species *A*2. For each species, there exist two valve views: one view shows an individual, hollow, cylindrical valve with one circular open end, a protruding outer rim, and a ringleiste (an internal ledge projecting into the valve interior from the valve wall) (Fig. 1a,c). The second view shows a chain of two cylindrical valves linked by spines (Fig. 1b,d). The valve faces for both species are generally flat with one or more rings of round areolae (Supplementary Fig. 3a), or scattered areolae (Supplementary Fig. 3b). While the overwhelming majority (>99.9%) of the frustules are centric with radial symmetry and belong to the genus *Aulacoseira* (Fig. 1a–d), pennate diatom frustules with bilateral symmetry (such as the genus *Staurosirella*[1] frustule in Supplementary Fig. 4a) and sieve-like silica plates (Supplementary Fig. 4b) were also found in the sample.

During CVD, hydrocarbon species in the vapor infiltrate into all the frustule's surfaces, including the fine feature (e.g., channels, nanorods, *etc.*) surfaces inside the frustule wall, and form a continuous graphene coating that precisely preserves the frustule structure, as the schematic diagram illustrated in Fig. 1f. Subsequent dissolution of the silica in hydrofluoric acid leaves behind a free-standing graphene replica of the native frustule. As depicted in Fig. 1f, both the solid nanorods inside the areola and the hollow channels in the frustule wall are converted into tube-like structures in the resulting graphene replica.

Morphologies and interior structures of graphene replicas. Figure 2a,b shows the scanning electron microscopy (SEM) images of two typical graphene replicas derived from an individual valve of species *A*1 frustule and two linked valves of species *A*2 frustule, respectively. The free-standing graphene replicas retain the exact, 3D, cylindrical morphology as well as the characteristic surface features of the native frustules, such as the areolae on valve surfaces (Fig. 2a,b) and valve faces (Supplementary Fig. 5), the valve rim (Supplementary Fig. 6), the ringleiste (Supplementary Fig. 7), and the linking spines (Supplementary Fig. 8). Due to the thin, conductive nature of the graphene coating, some shallow interior structures of the replicas can be seen even in low-accelerating voltage (20 KeV) SEM imaging (Fig. 2c and Supplementary Figs. 7 and 8).

Figure 2d shows a species *A*2 graphene replica whose outer graphene coating was torn off during etching, leaving pores associated with the areolae. This unique graphene replica provides valuable insights into the interior structures of the species *A*2 frustules. High-magnification SEM imaging reveals that the replica's interior contains a complex network of interconnected graphene nanotubes

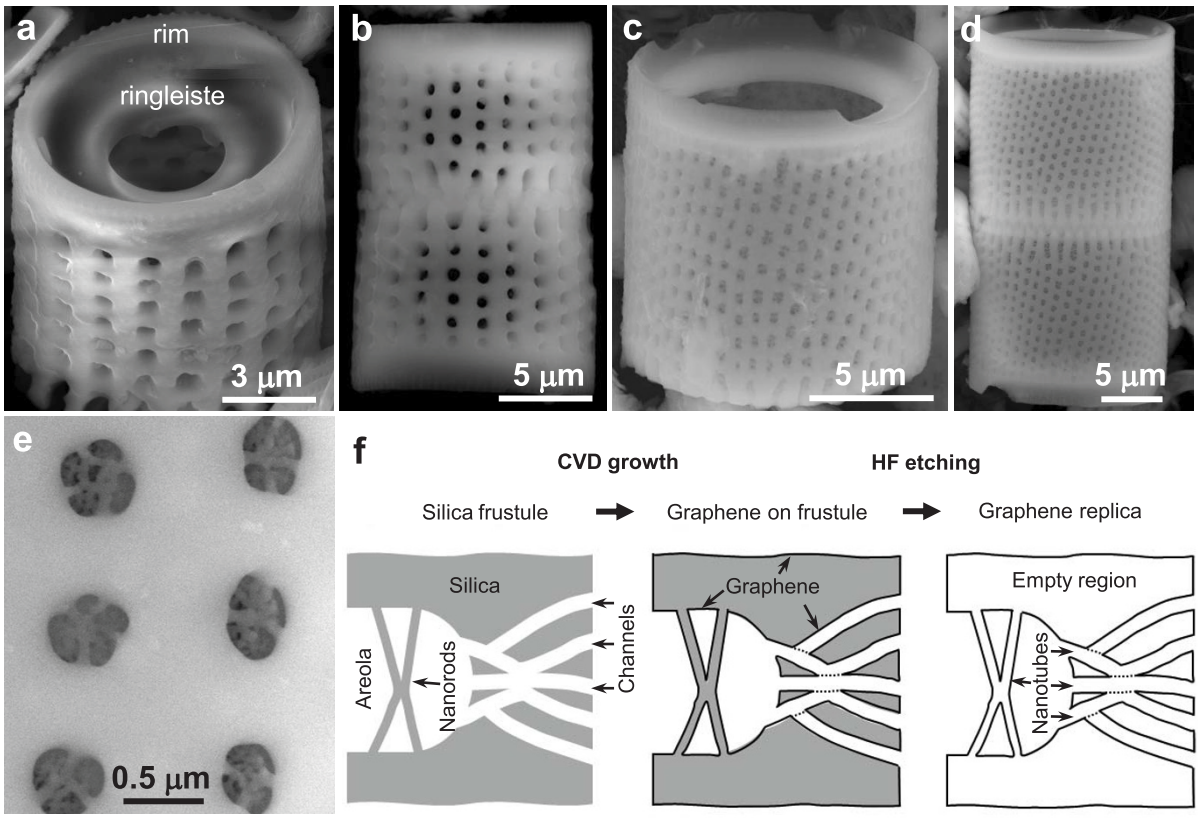

Figure 1 | SEM images of the genus *Aulacoseira* diatom frustules and the making of graphene replica. (a), A species *A*1 individual valve. (b), Two linked species *A*1 valves. (c), A species *A*2 individual valve. (d), Two linked species *A*2 valves. (e), High-magnification image of a species *A*2 valve showing the fine structures in areolae. (f), Schematic diagram showing how graphene replicas are formed using *Aulacoseira* diatom frustule as template. The drawing of the frustule valve is simplified by showing just one areola and the features associated with it.

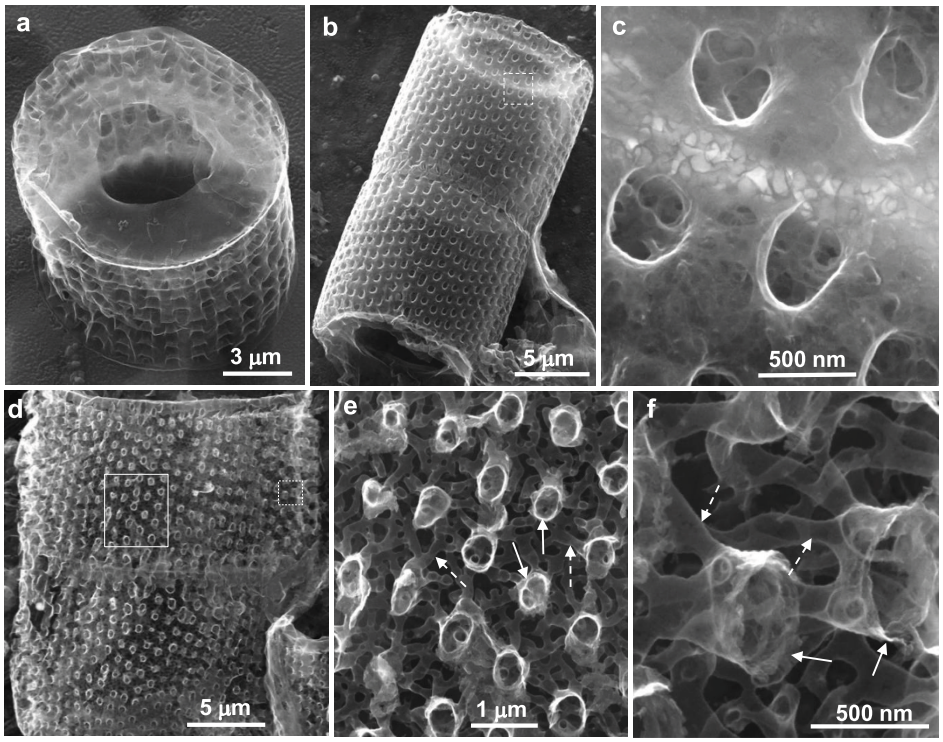

Figure 2 | SEM images of graphene replicas derived from the genus *Aulacoseira* diatom frustules. (a), A species *A*1 individual graphene valve. (b), Two linked species *A*2 graphene valves. (c), Enlarged image of the box area in b. (d), Low-magnification image of two linked species *A*2 graphene valves with the outer graphene coating torn off during etching. (e), Enlarged image of the solid-line box area in d. (f), Enlarged image of the dashed-line box area in d. In e and f, the solid-line white arrows indicate the positions of areolae, and the dashed-line white arrows indicate the interconnected nanotubes. The empty regions between the areolae and between the nanotubes were solid silica in the native frustule.

with various diameters (50–150 nm; as indicated by the dashed-line white arrows in Fig. 2e,f). Such complex nanotube networks are also observed in cross-sectional imaging experiments (Supplementary Fig. 9). The nanotube network meanders throughout the wall of the replica, connecting the pores on the frustule's inner surface with the areolae on the frustule's outer surface. Since the graphene nanotubes were formed by depositing carbon on the inner surfaces of the channels (see Fig. 1f), these species *A*2 graphene replicas provide the first evidence for the existence of an internal, interconnected network of channels in the species *A*2 frustule. These channels link the frustule's internal space, containing the diatom cell, with its external environment. Such channel networks could not possibly have been discovered by imaging the opaque silica frustules. Indeed, observations of the cross section of a broken species *A*2 frustule showed a seemingly simple porous wall structure (see Supplementary Fig. 2b) rather than a complicated network of interconnected channels.

The morphologies and interior structures of the *Aulacoseira* graphene replicas were further studied using a scanning transmission electron microscope (STEM) in both the SEM and transmission electron microscopy (TEM) modes. The STEM images in the SEM mode confirm the preservation of the morphology and surface features of the native frustules (Fig. 3a; see also Supplementary Fig. 10a,c–f and Supplementary Fig. 11a,d). Remarkably, in the TEM mode the micron-sized graphene replicas are highly transparent (Fig. 3b; see also Supplementary Fig. 10b and Supplementary Fig. 11b,c,e), enabling, for the first time, the entire interior structure of a diatom frustule to be visualized. With this TEM imaging mode it becomes clear that the *Aulacoseira* valves have a vase-like internal profile. The bottom of the graphene vase is convex. The body, which is the inner surface of the frustule wall, has either a convex side (Fig. 3b; the vase body in this replica has a bulbous shape) or a straight side (Supplementary Fig. 10b and Supplementary Fig. 11b,e; the vase bodies in these replicas have a cylinder shape). The neck, which was formed by coating the inner rim of the frustule's ringleiste, has a diameter of about one-third to one-half of the outer diameter of the frustule. The neck generally has concave sides. The lip, which was formed along the inward surface of the frustule's protruding rim, is smoothly curved in and connected with the outer surface of the cylindrical replica at the top. Besides the connection at the top, the vase and the outer cylinder of the replica are connected and support each other by either large, straight, cylindrical graphene areolae (for species *A*1) or an interconnected, small graphene nanotube network (for species *A*2). Moreover, TEM imaging on species *A*2 replicas (Fig. 3c) provides further evidence for the existence of an interconnected network of channels in the species *A*2 frustules.

The present shape-preserving CVD technique has distinguished and revealed two species of *Aulacoseira* diatoms with very different internal frustule structures. Particularly, the high penetration and uniform deposition of gaseous hydrocarbons in the complex inner channel networks of the species *A*2 frustules clearly demonstrates the CVD technique's unique value in the exploration of the interior fine features of diatom frustules. In addition to the putative *Aulacoseira* frustules replicated, frustules of a pennate genus, *Staurosirella,* and sieve-like plates were also replicated, as the examples shown in Supplementary Fig. 12 and Supplementary Fig. 13, respectively. The images of the sieve plate replicas further emphasize the unique ability of the CVD technique to reveal complexity in seemingly simple structures. The unique bottle shape of the pores, with two open ends connecting the surfaces of the plate, in the sieve plate could never have been predicted from an external view.

The unexpected internal structures revealed in these graphene replicas may have profound impacts on our understanding of how diatoms make their shells and how diatom cells interact with their external environment. For example, the two species of *Aulacoseira* diatoms with very different internal frustule structures imply that

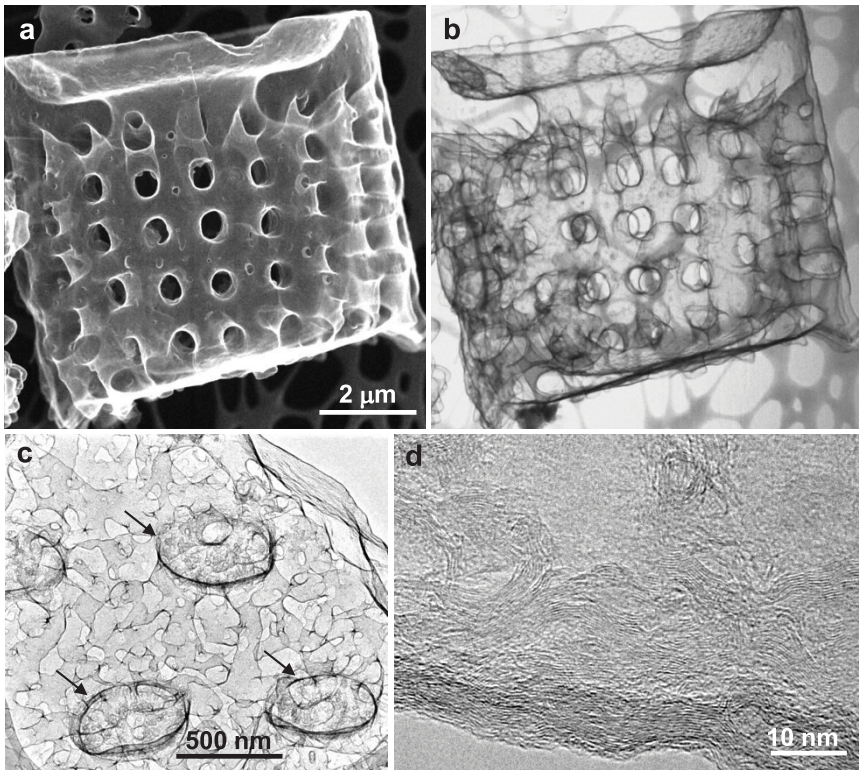

Figure 3 | STEM and HRTEM images of graphene replicas derived from *Aulacoseira* frustules. (a),(b), STEM images of a species *A*2 replica taken in the SEM mode and TEM mode, respectively. (c), TEM image of a piece of a species *A*2 replica with the open ends of the areolae (indicated by black arrows) facing out of the plane of view. (d), HRTEM image of graphene coating.

these two *Aulacoseira* cells may interact with the external environment in very different ways. Although species *A*1 has a relatively direct physical connection with its environment, species *A*2 has a convoluted network of channels which must be navigated between entering the cell wall and reaching the cell membrane. The presence of this channel network may imply that species *A*2 cells have specific osmoregulatory needs. It is well known that pore size impacts the attraction of particles of different sizes to enter into synthetic systems[14]. This may support the idea that species *A*2 is using its channel network, with its varying diameters, in order to select for or against osmolytes of certain sizes.

Microstructures and Raman spectroscopy of catalyst-free CVD graphene. The microstructures and quality of the graphene grown on silica frustules by metal-catalyst-free CVD were examined using high-resolution TEM (HRTEM) and Raman spectroscopy. HRTEM imaging shows that the graphene coating is fairly graphitized even though no metal catalysts were used. The coating typically consists of 5–10 graphene layers (Fig. 3d). Raman spectra acquired on individual graphene replicas reveal the presence of D (~1358 cm^{-1}), G (~1588 cm^{-1}), 2D or G' (~2693 cm^{-1}), and D+D' (~2928 cm^{-1})[15] bands (Fig. 4). The well-resolved G band along with the strong intensity of the 2D (G') band indicates the presence of significant sp^2 carbon in the replica. The broad 2D band and the relatively low ratio of 2D band intensity to that of the G band (I_{2D}/I_G = 0.91 for the spectrum in Fig. 4) reveal that the graphene coating contains multi-layers. The high intensity of the D band, however, suggests the presence of a relatively high level of disorder in the graphene replica, which is consistent with the HRTEM results. It is worth noting that the quality of the metal-catalyst-free CVD graphene grown on silica substrates is comparable to that of the metal-catalyzed CVD multiwall carbon nanotubes[16].

Discussion

We demonstrate that quality graphene can be grown on silica surfaces using methane CVD without the presence of metal catalysts. CVD growth of graphene on non-metal substrates has gained increased attention[17–19]. Compared with the dominant metal-catalyzed CVD growth[20,21], the metal-catalyst-free CVD allows the growth of graphene on technologically important dielectric substrates (such as SiO_2) for direct device fabrication, avoiding the need for a complicated postgrowth transfer process. However, unlike the well-developed metal-catalyzed CVD, understanding of the growth

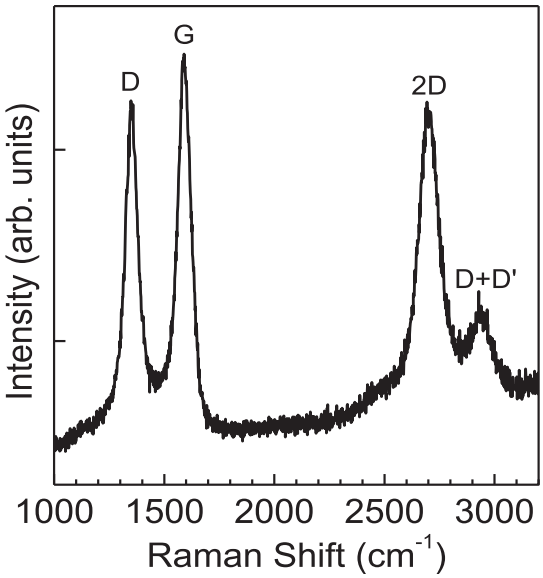

Figure 4 | Raman spectrum acquired on an individual graphene replica.

mechanism on non-metal surfaces is very limited[17–19]. We recently reported conformal growth of graphene layers on inactive carbon basal planes of carbon nanotubes using metal-catalyst-free CVD of methane[22]. That study reveals that at sufficiently high temperature (~1,100–1,200 °C) metal is not indispensable in graphene growth and carbon can self-assemble into a hexagonal network on existing carbon surfaces via a two-step of nucleation and growth process[23,24]. Since the synthesis conditions in the present growth on silica surfaces is very similar to that on carbon basal planes, it is expected that the graphene growth on the silica frustules also follows the two-step carbon deposition mechanism[22]. Owing to the high penetration of the gaseous hydrocarbons, growth occurs uniformly on all the fine feature surfaces (see Fig. 1f) in the frustules, thus forming a continuous and uniform graphene coating that precisely preserves the morphologies and fine features of the frustules.

This work demonstrates the fabrication of a new type of complex graphene architecture – 3D graphene micro-assemblies (replicas) with unprecedented intricate nanoscale patterns inherited from the natural diatom frustules – by simple methane CVD. Considering the enormous varieties of diatom species, this fabrication strategy enables the synthesis of various types of graphene replicas with species-specific patterns. Since each diatom species has extraordinary reproduction capability (a single diatom can produce approximately 100 million descendants within a month)[25,26], the present shape-preserving CVD method enables large quantities of the same 3D graphene replicas with precisely controlled microscale shapes and nanoscale features to be fabricated. The transparency of the graphene replicas to electron beam allows the interior and entire 3D structures to be visualized, overcoming the previous limitation of only imaging surface morphology. The electrically transparent graphene replicas provide a new way for the investigation of frustule morphology and thus provide insights for the study and understanding of frustule morphogenesis. The understandings thus obtained could impact the understanding of diatom biology and physiology, and could lead to substantial benefits in a wide range of important areas where diatoms are concerned, from nanotechnology to climate change[3–9]. Finally, the present study establishes a method to grow quality graphene on silica substrates based on metal-catalyst-free CVD. Besides on the natural, biological silica templates as diatom frustules, our extended experiments showed that graphene can also be grown on synthetic silica substrates such as silica beads, porous silica, and silica wafers.

Methods

Purification of diatom frustules. 12 g diatomaceous earth sample (Earthworks Health LLC, Norfolk, NE) was ultrasonically dispersed in 500 mL DI water for 10 min. The mixture was settled for 5 min to remove large impurities (as sediment). The above procedure was repeated for 3 times. The final suspension containing diatom frustules was dried in a rotary evaporator at 140°C under vacuum. The dried frustules were heated to 600°C for 8 h to remove the residual organic materials. The calcinated frustules were then suspended in 500 DI water and settled for 4 h to remove the frustule debris (in suspension). The final sediment containing high-purity diatom frustules was dried and used for graphene growth.

Fabrication of graphene replicas. Purified diatom frustules were spread on either aligned carbon nanotube sheets (~6 mm long and 10 mm wide)[27] or Si wafer (~10 mm long and 10 mm wide). The nanotube sheets or Si wafer were fixed vertically on a graphite beam which was then inserted into a horizontal tube furnace for graphene growth. The metal-catalyst-free CVD growth of graphene on frustule surfaces requires a growth temperature of around 1,150 °C. Below 1,100 °C graphene does not grow, and higher temperature (>1,200 °C) can result in the melting and thus destruction of the silica frustules. In present study, the growth temperature was 1,150 °C. Other synthesis parameters were: methane flow rate, 10 standard cubic centimeters per minute (sccm); Ar flow rate, 150 sccm; growth chamber pressure, 50 Torr; and growth time, 5–10 min. After growth, the samples were immersed in a 1 M HF aqueous solution for 2 h to completely dissolve the silica shells, followed by washing in methanol and drying in an oven at ~80 °C for 1 h. It is worth noting that if the graphene coating is very thin (mainly caused by short growth time), the graphene replica will be too weak to maintain its integrity, tending to collapse in the etching process (see Supplementary Fig. 14).

Characterization methods. The morphologies and structures of the graphene replicas were characterized by a SEM (FEI Inspect F FEG SEM) and a STEM (Hitachi HF-3300 FEG TEM/STEM). In preparing STEM specimens, the graphene replicas were dispersed in methanol and a drop of the suspension was dispersed onto a lacy copper grid.

Raman spectra of individual graphene replicas were acquired with a Renishaw Raman 1000 system equipped with an integrated Leica microscope. The 514 nm excitation light from an argon ion laser was focused to 5 μm spot using a 50× microscope objective. The laser power at the sample was approximately 1 mW.

1. Spaulding, S. A., Lubinski, D. J. & Potapova, M. Diatoms of the United States (2010). http://westerndiatoms.colorado.edu Date of access: 08/01/2013.
2. Round, F. E., Crawford, R. M. & Mann, D. G. *The diatoms, biology & morphology of the genera.* (Cambridge University Press, 1990).
3. Hildebrand, M. Diatoms, biomineralization process, and genomics. *Chem. Rev.* **108**, 4855–4874 (2008).
4. Gross, M. The mysteries of the diatoms. *Curr. Biol.* **22**, R581–R585 (2012).
5. Bradbury, J. Nature's nanotechnologists: unveiling the secrets of diatoms. *PLoS Biol.* **2**, 1512–1515 (2004).
6. Gordon, R., Losic, D., Tiffay, M. A., Nagy, S. S. & Sterrenburg, F. A. S. The glass menagerie: diatoms for novel applications in nanotechnology. *Trends Biotechnol.* **27**, 116–127 (2008).
7. Street-Perrot, F. A. & Barker, P. A. Biogenic silica: a neglected component of the coupled global continental biogeochemical cycles of carbon and silicon. *Earth Surf. Process. Landf.* **33**, 1436–1457 (2008).
8. Field, C. B., Behrenfeld, M. J., Randerson, J. T. & Falkowski. Primary production of the biosphere: integrating terrestrial and oceanic components. *Science* **281**, 237–240 (1998).
9. Armbrust, E. V. The life of diatoms in the world's oceans. *Nature* **459**, 185–192 (2009).
10. Bao, Z. B. *et al.* Chemical reduction of three-dimensional silica micro-assemblies into microporous silicon replicas. *Nature* **446**, 172–175 (2007).
11. Scheffel, A., Poulsen, N., Shian, S. & Kröger, N. Nanopatterned protein microrings from a diatom that direct silica morphogenesis. *Proc. Natl. Acad. Sci. USA* **108**, 3175–3180 (2010).
12. Hildebrand, M., Kim, S., Shi, D., Scott, K. & Subramaniam, S. 3D imaging of diatoms with ion-abrasion scanning electron microscopy. *J. Struct. Biol.* **166**, 316–328 (2009).
13. Hildebrand, M., Doktycz, M. J. & Allison, D. P. Application of AFM in understanding biomineral formation in diatoms. *Eur. J. Physiol.* **456**, 127–137 (2008).
14. Beck, R. E. & Schultz, J. S. Hindered diffusion in microporous membranes with known pore geometry. *Science* **170**, 1302–1305 (1970).
15. Dresselhaus, M. S., Jorio, A., Hofmann, M., Dresselhaus, G. & Saito, R. Perspectives on carbon nanotubes and graphene Raman spectroscopy. *Nano Lett.* **10**, 751–758 (2010).
16. Antunes, E. F., Lobo, A. O., Corat, E. J. & Trava-Airoldi, V. J. Influence of diameter in the Raman spectra of aligned multi-walled carbon nanotubes. *Carbon* **45**, 913–921 (2007).
17. Chen, J. Y. *et al.* Oxygen-aided synthesis of polycrystalline graphene on silicon dioxide substrates. *J. Am. Chem. Soc.* **133**, 17548–17551 (2011).
18. Hong, G., Wu, Q. H., Ren, J. G. & Lee, S. T. Mechanism of non-metal catalytic growth of graphene on silicon. *Appl. Phys. Lett.* **100**, 231604 (2012).
19. Chen, J. Y. *et al.* Two-stage metal-catalyst-free growth of high-quality polycrystalline graphene films on silicon nitride substrates. *Adv. Mater.* **25**, 992–997 (2013).
20. Li, X. S. *et al.* Large-scale synthesis of high-quality and uniform graphene films on copper foils. *Science* **324**, 1312–1314 (2009).
21. Kim, K. S. *et al.* Large-scale pattern growth of graphene films for stretchable transparent electrodes. *Nature* **457**, 706–710 (2009).
22. Li, K. Y. *et al.* Self-assembly of graphene on carbon nanotube surfaces. *Sci. Rep.* **3**, 2353 (2013).
23. Oberlin, A. Pyrocarbons. *Carbon* **40**, 7–24 (2002).
24. Hu, Z. J. & Hüttinger, K. J. Mechanisms of carbon deposition—a kinetic approach. *Carbon* **40**, 624–628 (2002).
25. Toster, J. *et al.* Regiospecific assembly of gold nanoparticles around the pores of diatoms: toward three-dimensional nanoarrays. *J. Am. Chem. Soc.* **131**, 8356–8357 (2009).
26. Miron, A. S., Gomez, A. C., Camacho, F. G., Grima, E. M. & Chisti, Y. Comparative evaluation of compact photobioreactors for large-scale monoculture of microalgae. *J. Biotechnol.* **70**, 249–270 (1999).
27. Gu, Z. J. *et al.* Aligned carbon nanotube-reinforced silicon carbide composites produced by chemcial vapor reaction. *Carbon* **49**, 2475–2482 (2011).

Acknowledgments

Z.W.P. thanks the support of a NSF CAREER grant (DMR-0955908). Work by M.H. and S.L. was supported by an AFOSR MURI award (RF00965521). Work by S.D. and S.M.M. was supported by the Chemical Sciences, Geosciences and Biosciences Division of Basic Energy Sciences (BES), U.S. Department of Energy (DOE). The TEM characterization was

conducted at the Oak Ridge National Laboratory ShaRE User Facilities, which is sponsored by the Division of Scientific User Facilities of BES, U.S. DOE.

Author contributions

Z.W.P. conceived and designed the experiments. L.X., X.F.L. and Z.W.P. fabricated the graphene replicas and conducted SEM characterizations. Z.W.P., J.Y.H. and Y.-J.C. performed TEM characterizations. M.H. and S.L. analyzed the implications of graphene replicas on frustule morphogenesis. Y.-J.C. purified diatom frustules. S.M.M. and S.D. conducted Raman measurements and analysis. Z.W.P., M.H. and S.L. wrote the manuscript. All authors discussed the results and commented on the manuscript.

Additional information

Supplementary information accompanies this paper at http://www.nature.com/scientificreports

Competing financial interests: The authors declare no competing financial interests.

How to cite this article: Pan, Z.W. *et al*. Electronically transparent graphene replicas of diatoms: a new technique for the investigation of frustule morphology. *Sci. Rep.* **4**, 6117; DOI:10.1038/srep06117 (2014).